Discovery of FLT3 inhibitors for the treatment of acute myeloid leukemia

Grimm, S.H.

Chapter 4

Discovery of new mutant-active FLT3 inhibitors by high throughput screening*

Introduction

Acute myeloid leukemia (AML) is a disorder of hematopoietic stem-cells, in which during hematopoiesis cell differentiation is impaired, leading to immature blood cells flooding the bloodstream.[1] If untreated, this malignancy leads to death within weeks to months, especially for older patients who cannot cope with the severe standard chemotherapy treatment.[1] Several genetic alterations have been discovered, among them an internal tandem duplication (ITD) in the juxtamembrane domain of the Fms-like tyrosine kinase 3 (FLT3) receptor.[2] This mutation, FLT3-ITD, has been identified as a driver mutation in cancer progression, enabling growth factor independent cell proliferation.[3–5] This led to an extensive effort to discover FLT3 inhibitors for the use in AML treatment,[6,7] which resulted in the recent approval of midostaurin for treatment of AML patients with FLT3-ITD mutations. Other clinically investigated drugs, such as sorafenib or quizartinib, suffered from the emergence of treatment resistant clones possibly due to evolutionary selection during inhibitor treatment.[8–12] Several of these mutations that impaired the drug binding to the FLT3 kinase domain were identified, affecting binding affinity by either direct exchange of amino acids interacting with the drug (F691 mutations)[12,13], or a structural resistance, destabilizing the conformation the FLT3 kinase domain that is binding to the drug (D835 mutations)[11,13,14]. A schematic representation of the location of these mutations within the FLT3 receptor is shown in Figure 1.

* The data presented in this chapter was gathered in collaboration with Ruud H. Wijdeven, Jan van Groningen, Helma Rutjes, Constant A. A. van Boeckel, Herman S. Overkleeft, Jacques Neefjes and Mario van der Stelt.

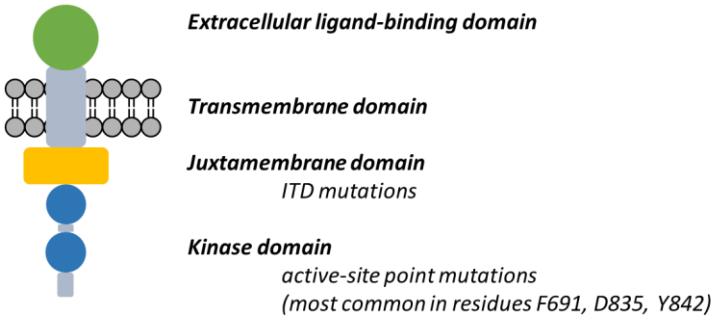

Figure 1: Schematic representation of the FLT3 receptor.

Since molecules rely on specific interactions with an enzyme for effective inhibition, it is unlikely that one single drug can counter all potential mutations that confer resistance to different drugs. This exemplifies the need for multiple structurally diverse chemotypes to treat AML that are active against wild type FLT3 as well as currently known mutations of FLT3, to successfully treat AML.

To this end, a screening strategy was devised to identify such new molecules. In the first stage a high throughput screen (HTS) was performed to identify novel inhibitors of wild type FLT3. After triaging, a selected set of hits was tested on cell lines, to ensure cellular activity as well as activity against cell lines carrying FLT3 F691 and D835 mutants.

To confirm cellular activity of compounds, MV4-11 cells were used which originated from a patient with biphenotypic B-myelomonocytic leukemia. Its proliferation is FLT3-signaling dependent and continuous inhibition of FLT3 in MV4-11 cells over several days leads to apoptosis.[4] To check for general off-target activity, the U937 cell line was chosen, which does not depend on FLT3 signaling. U937 cells are hematopoietic cells derived from a patient with histiocytic lymphoma.[15] Here, treatment with selective FLT3 inhibitors is not expected to lead to apoptosis.

To investigate the effects of mutant FLT3 Ba/F3 cells are used. Ba/F3 is a murine hematopoietic cell line dependent on the presence of interleukin 3 (IL-3) for proliferation.[16] However, Ba/F3 cell proliferation can be rendered IL-3 independent by using retroviruses to induce the stable expression of constitutively active tyrosine kinase or other oncogenes.[17] This oncogene-dependent signaling was exploited to generate Ba/F3 cell lines dependent on FLT3-ITD and/or F691L, D835H and D835Y point mutants.[16,18] The Ba/F3 wild type and the Ba/F3 FLT3-ITD variations were used to further profile the hits.

Results and Discussion

In vitro screening campaign

A fluorescence resonance energy transfer (FRET) based assay, using recombinantly expressed kinase, was used to screen for FLT3 active molecules (Figure 2A).[19] After adaption of the assay for a 1,536 well plate format, the search for new chemical entities was started by screening a library of 231,152 compounds against wild type-FLT3 in 3 days at a concentration of 10 µM. The results from the *in vitro* screening as well as the selection criteria are summarized in Figure 3. The quality of the data was ensured by monitoring Z' and S/B per plate. These showed that the assay is robust with values of ~0.8 and 6-13, respectively. 4,262 primary active compounds were found using cut-off criteria of a Z-score of ≤ -4 (~20-25% effect). The primary actives were retested in the same assay (Z-score of ≤ -4 corresponding to ~35% effect). This resulted in 1,400 confirmed actives, which corresponds to a hit rate of 0.61%.

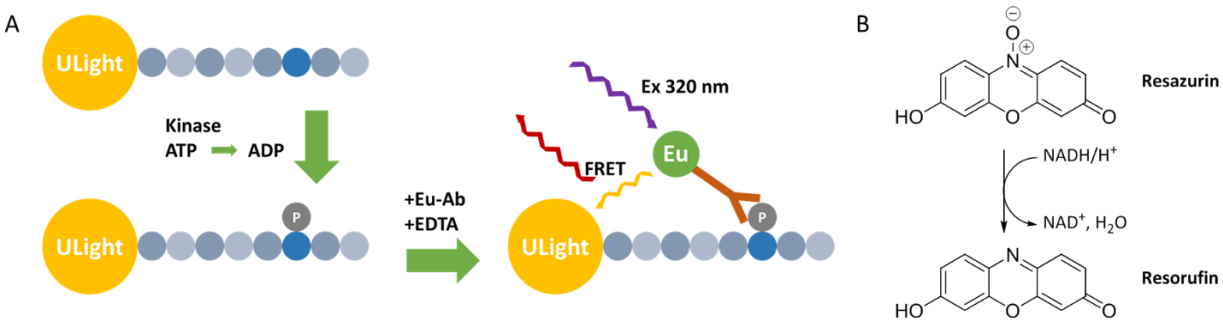

Figure 2: Used assays in the screening process: (A) Schematic representation of the used commercial FRET-based FLT3 *in vitro* assay. A peptide chain, tagged with an ULight acceptor fluorophore is phosphorylated by the kinase. Subsequent addition and binding of an europium donor fluorophore-tagged antibody, specific for the phosphorylated peptide brings donor and acceptor into close proximity, enabling FRET measurement. (B) The resazurin/resorufin redox reaction, the basis of the used alamarBlue cell viability assay is dependent on metabolic activity of the tested cells.

To further reduce the number of hits and to deprioritize pan-kinase inhibitors, deselection assays were performed against RAC-alpha serine/threonine-protein kinase (AKT1) and cAMP-dependent protein kinase (PKA) at 1.25 and 12.5 µM. In the deselection assay only 34 and 9 compounds showed activity of > 40% against AKT1 and PKA, respectively. These compounds were removed from the list. Subsequent analysis of the hit list for common pan-assay interference compounds (PAINS)[20,21] and intellectual property (IP) situation resulted in 141 compounds.

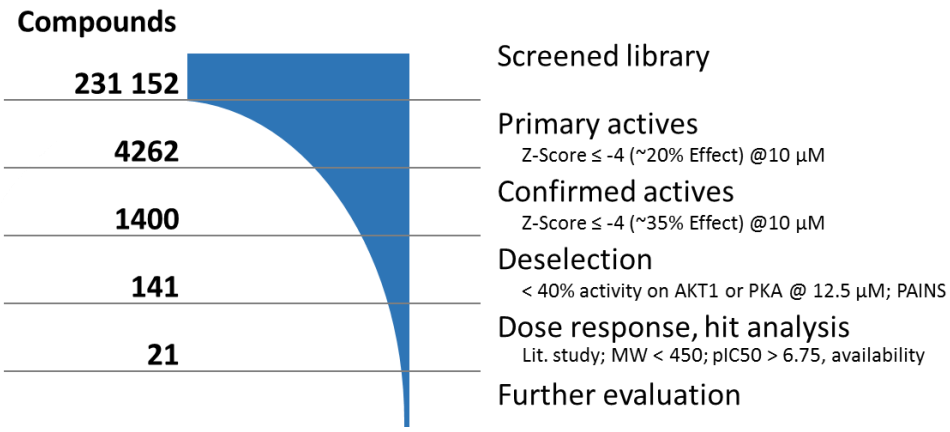

Figure 3: Hit triaging during the high-throughput screening.

The remaining 141 compounds were tested in a dose-response assay against FLT3 to determine inhibitory potency, followed by a detailed literature analysis for known kinase activity and freedom-to-operate with respect to IP. After further analysis of compound availability and purity, compounds were selected on basis of the following cut-offs: MW < 450; FLT3 pIC_{50} > 6.5. This resulted in a list with 21 compounds (Table 1).

Cellular evaluation of the qualified hit list

The 21 selected hits were further profiled in proliferation assays using seven different cell lines (MV4-11, U937, Ba/F3, Ba/F3-FLT3-ITD and Ba/F3 with FLT-ITD with the following mutations F691L, D835H and D835Y). The alamarBlue proliferation assay is based on the metabolic redox conversion of the dye resazurin to resorufin in living cells (Figure 2B).[22,23] The results of this study are shown in Table 1. This qualified hit list shows a diverse set of kinase inhibitors, including crenolanib (**19**), a known FLT3 inhibitor, which was added as positive control. On basis of this data, as well as the *in vitro* potency and general physicochemical properties, the hit list was carefully analyzed to make a selection of compounds exhibiting a balanced profile that could be further optimized.

The list includes compounds, such as **18**, that showed almost equal activity against all cell lines, regardless of FLT3 dependency, suggesting off-target mediated cytotoxicity. These compounds were not further considered. In addition, other compounds (e.g. **2**, **8** and **17)** were deselected based on their low cellular activity in the FLT3 dependent cell lines (pIC_{50} < 6).

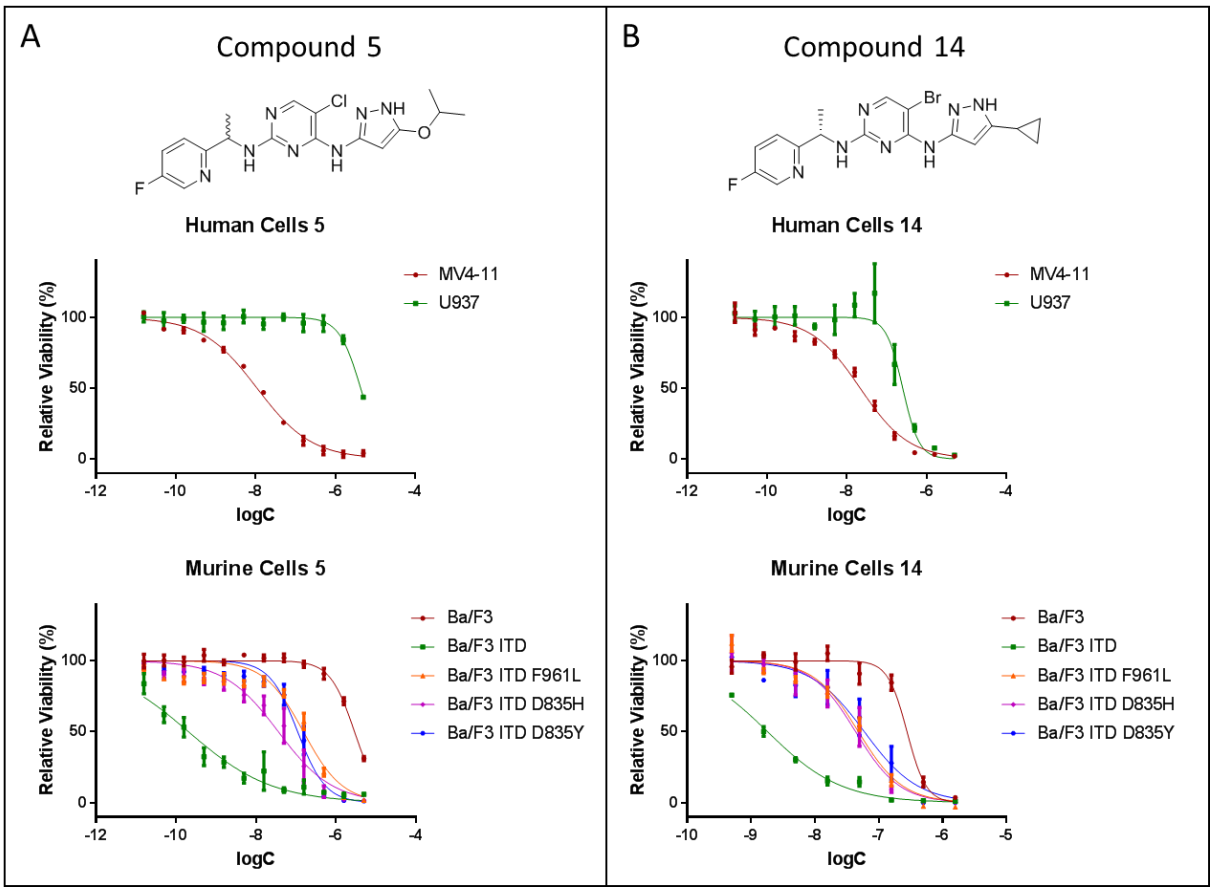

Figure 4: Summary of activity data of the selected hit compounds. Dose-response curves show individual data points ± SEM.

Finally, hits **5** (SPCE000476_01, 5-chloro-N^2-(1-(5-fluoropyridin-2-yl)ethyl)-N^4-(5-isopropoxy-1*H*-pyrazol-3-yl)pyrimidine-2,4-diamine, Figure 4A) and **14** (NP_004099_001, (*S*)-5-bromo-N^4-(5-cyclopropyl-1*H*-pyrazol-3-yl)-N^2-(1-(5-fluoropyridin-2-yl)ethyl)pyrimidine-2,4-diamine, Figure 4B) were selected for further hit optimization (Chapter 5) on basis of their high activity against ITD mutations (MV4-11 and Ba/F3-ITD), acceptable point-mutant activity and good physico chemical parameters, such as low molecular weight (**5**: 392 and **14**: 418 g/mol) and satisfactory LipE (**5**: 4.9 and **14**: 4.4).

Conclusion

More than 231,000 compounds have been successfully screened in a 1,536-well format against wildtype FLT3. After hit confirmation and two deselection assays against AKT1 and PKA a dose-response assay was performed with 141 hit compounds, resulting in a qualified hit list of 21 compounds. These compounds were further evaluated on their anti-proliferative effects on seven cell lines. This led to the selection of compounds **5** and **14**, which displayed the most optimal profile and structure for further optimization (Chapter 5).

Table 1: Summary of the 21 molecules as FLT3 inhibitors, which were in-depth evaluated. *In vitro* pIC_{50} FLT3 was measured using a FRET based assay, all other pIC_{50}-values are effects on cell proliferation, measured using the alamarBlue viability assay, based on a resazurin/resorufin redox reaction. cLogP and tPSA were calculated with PerkinElmer ChemDraw 16. LipE = pIC_{50} (*in vitro* FLT3) – cLogP.

			pIC_{50} ± SEM										
						Ba/F3							
Entry	**Code**	**Structure**	***in vitro* FLT3**	**MV4-11**	**U937**	***wt***	**FLT3 ITD**	**FLT3 ITD F691L**	**FLT3 ITD D835H**	**FLT3 ITD D835Y**	**MW (Da)**	**cLogP**	**LipE**	**tPSA (Å²)**
1	SPCE000338_01	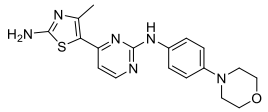	7.6	7.9 ± 0.1	6.5 ± 0.1	6.5 ± 0.1	7.0 ± 0.1	7.4 ± 0.1	6.9 ± 0.1	6.8 ± 0.1	368	2.5	5.0	88
2	SPCE000368_01	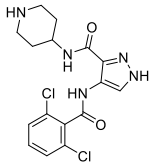	6.8	6.7 ± 0.1	6.8 ± 0.1	5.7 ± 0.1	6.0 ± 0.1	6.2 ± 0.1	6.0 ± 0.1	5.9 ± 0.1	382	0.3	6.5	95
3	SPCE000415_01	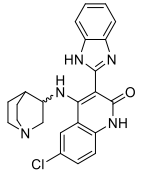	8.5	9.6 ± 0.1	7.6 ± 0.1	7.2 ± 0.1	9.5 ± 0.1	8.2 ± 0.1	9.0 ± 0.1	8.6 ± 0.1	420	4.0	4.4	69
4	SPCE000442_01	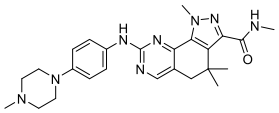	7.9	8.1 ± 0.1	6.4 ± 0.1	6.4 ± 0.1	8.5 ± 0.1	7.2 ± 0.1	7.4 ± 0.1	7.0 ± 0.1	461	3.1	4.9	88
5	SPCE000476_01	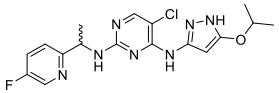	8.4	8.0 ± 0.1	5.4 ± 0.1	5.5 ± 0.1	9.7 ± 0.1	6.8 ± 0.1	7.4 ± 0.1	7.0 ± 0.1	392	3.5	4.9	95

Entry	Code	Structure	pIC50 ± SEM								MW (Da)	cLogP	LipE	tPSA (Å²)
			in vitro FLT3	MV4-11	U937	Ba/F3								
						wt	FLT3 ITD	FLT3 ITD F691L	FLT3 ITD D835H	FLT3 ITD D835Y				
6	NP_000948_001	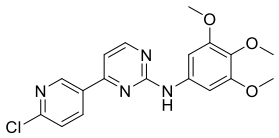	7.2	6.7 ± 0.1	6.5 ± 0.1	6.2 ± 0.1	6.8 ± 0.1	6.5 ± 0.1	6.4 ± 0.1	6.2 ± 0.1	373	3.0	4.3	77
7	SPCA067086_01	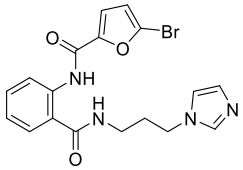	7.1	7.1 ± 0.1	< 5	< 5	7.0 ± 0.1	6.0 ± 0.1	6.8 ± 0.1	6.9 ± 0.1	417	2.3	4.8	83
8	SPCA067975_01	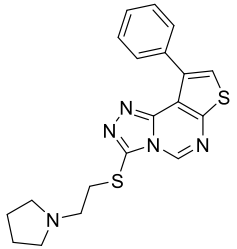	7.0	6.5 ± 0.1	< 5	< 5	6.3 ± 0.1	6.2 ± 0.1	6.2 ± 0.1	5.9 ± 0.1	382	3.8	3.2	44
9	CO_002775_001	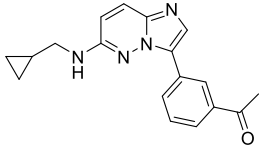	7.6	7.3 ± 0.1	5.6 ± 0.1	< 5	6.7 ± 0.1	< 5	6.5 ± 0.1	6.8 ± 0.1	306	3.3	4.3	57
10	NP_000412_001	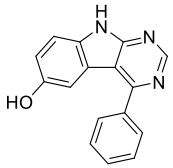	8.0	7.4 ± 0.1	5.8 ± 0.1	5.7 amb	7.3 ± 0.1	6.5 ± 0.1	7.2 ± 0.1	7.2 ± 0.1	261	3.5	4.5	57

Entry	Code	Structure	pIC$_{50}$ ± SEM								MW (Da)	cLogP	LipE	tPSA (Å^2)
			in vitro FLT3	MV4-11	U937	Ba/F3								
						wt	FLT3 ITD	FLT3 ITD F691L	FLT3 ITD D835H	FLT3 ITD D835Y				
11	NP_001016_001	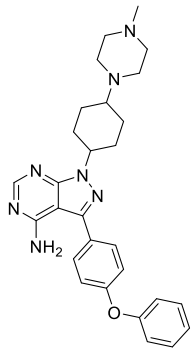	8.2	7.9 ± 0.1	5.4 ± 0.1	5.5 ± 0.2	7.3 ± 0.1	6.3 ± 0.1	6.9 ± 0.1	6.7 ± 0.1	484	3.6	4.6	82
12	NP_004035_001	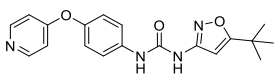	8.1	na	< 5	< 5	7.8 ± 0.2	6.3 ± 0.1	7.0 ± 0.1	6.5 ± 0.1	352	4.1	3.9	84
13	NP_004039_001	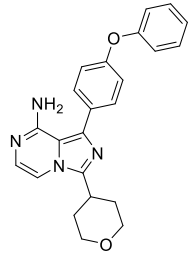	7.1	6.9 ± 0.1	5.2 ± 0.1	5.5 ± 0.3	6.8 ± 0.1	6.4 ± 0.1	6.6 ± 0.1	6.8 ± 0.1	386	4.4	2.7	72
14	NP_004099_001	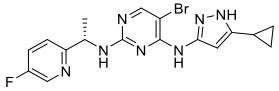	7.9	7.7 ± 0.1	6.6 ± 0.1	6.6 ± 0.1	8.7 ± 0.1	7.3 ± 0.1	7.4 ± 0.1	7.2 ± 0.1	418	3.5	4.4	86
15	SPCA043560_01	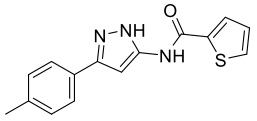	7.0	7.0 ± 0.1	5.0 ± 0.1	< 5	6.3 ± 0.1	6.1 ± 0.1	6.1 ± 0.1	6.0 ± 0.1	283	3.9	3.1	53

Entry	Code	Structure	pIC50 ± SEM							MW (Da)	cLogP	LipE	tPSA (Å²)
			in vitro FLT3	Ba/F3									
				MV4-11	U937	*wt*	FLT3 ITD	FLT3 ITD F691L	FLT3 ITD D835H	FLT3 ITD D835Y				
16	SPCA053729_01	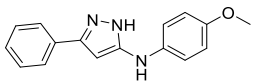	6.8	6.5 ± 0.1	< 5	< 5	6.1 ± 0.1	5.8 ± 0.1	5.4 ± 0.2	< 5	265	4.6	2.2	46
17	SPCE000191_01	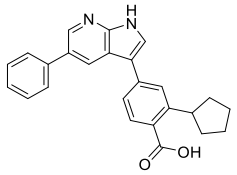	8.3	6.1 ± 0.1	5.8 ± 0.1	< 5	6.6 ± 0.1	5.6 ± 0.2	6.0 ± 0.1	6.1 ± 0.1	382	5.7	2.6	62
18	SPCE000396_01	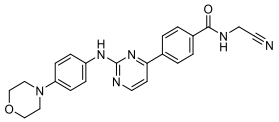	7.2	6.6 ± 0.1	6.2 ± 0.1	6.1 ± 0.1	6.5 ± 0.1	6.4 ± 0.1	6.3 ± 0.1	6.2 ± 0.1	414	2.2	5.0	102
19	SPCE000437_01	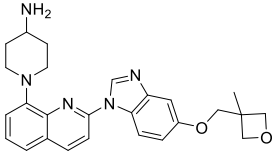	9.0	9.3 ± 0.1	5.8 ± 0.1	6.0 ± 0.1	8.4 ± 0.1	7.1 ± 0.1	7.7 ± 0.1	7.9 ± 0.1	444	3.4	5.6	76
20	SPCE000468_01	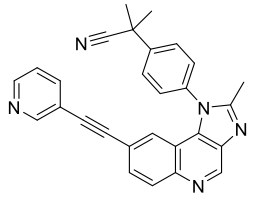	7.3	6.6 ± 0.1	7.0 ± 0.1	6.2 ± 0.2	6.6 ± 0.2	6.5 ± 0.1	6.5 ± 0.1	6.5 ± 0.1	428	5.5	1.8	64
21	SPCE000480_01	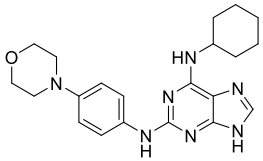	7.2	7.2 ± 0.1	6.9 ± 0.1	7.5 ± 0.5	7.8 ± 0.5	8.1 ± 0.7	8.2 ± 0.6	8.2 ± 0.6	393	4.9	2.3	86

Experimental

Final conditions primary screen and active confirmation

20 nL compound stock dissolved in DMSO or only DMSO were dispensed in a 1536 well plate (white polystyrene NBS microplate, Corning, cat# 3729). After addition of 2 µL assay buffer (50 mM HEPES (pH 7.5), 1 mM EGTA, 10 mM $MgCl_2$, 0.01% Tween-20, 2 mM DTT) and 2 µL 0.75 µg/mL FLT3 (BPS Bioscience, cat# 40225, lot# 141201) dissolved in assay buffer, the plate was centrifuged at 187 g for 30 s and incubated in the dark for 30 min. 2 µL of a mix of 600 µM ATP, 12.5 nM peptide (PerkinElmer; Lance® Ultra ULight™ TK-peptide; cat# TRFO127-M; lot# 1934454)) and 4 nM antibody (PerkinElmer; Lance® Eu-W1024-anti-phosphotyrosine(PT66); cat# AD0068;lot# 1889053) were added and the plate was again centrifuged at 187 g for 30 s and incubated in the dark for 90 min. The FRET was measured on a Envision plate reader (excitation: 337 nm, emission filter donor: 615 nm, emission filter: acceptor 665 nm).

Final conditions deselection assay AKT1

2.5 nL or 25 nL compound stock dissolved in DMSO or only DMSO were dispensed in a 1536 well plate (white polystyrene NBS microplate, Corning, cat# 3729). After addition of 2 µL assay buffer (50 mM HEPES (pH 7.5), 1 mM EGTA, 10 mM $MgCl_2$, 0.01% Tween-20, 2 mM DTT) and 2 µL 0.5 nmol/min AKT1 (SignalChem, cat# A16-10G-10, lot# W293-3) dissolved in assay buffer, the plate was centrifuged at 187 g for 30 s and incubated in the dark for 30 min. 2 µL of a mix of 200 µM ATP, 35 nM peptide (PerkinElmer; ULight™ phospho-40S-ribosomal protein S6 peptide; cat# TRF0129-D; lot# 1908909)) and 4 nM antibody (PerkinElmer; Eu-anti-phosph-rpS6, cat# TRF0217-D, lot# 1759011) were added and the plate was again centrifuged at 187 g for 30 s and incubated in the dark for 30 min. The FRET was measured on a Envision plate reader (excitation: 337 nm, emission filter donor: 615 nm, emission filter: acceptor 665 nm).

Final conditions deselection assay PKA

2.5 nL or 25 nL compound stock dissolved in DMSO or only DMSO were dispensed in a 1536 well plate (white polystyrene NBS microplate, Corning, cat# 3729). After addition of 2 µL assay buffer (50 mM HEPES (pH 7.5), 1 mM EGTA, 10 mM $MgCl_2$, 0.01% Tween-20, 2 mM DTT) and 2 µL 3.2 nmol/min PKAcα (SigalChem, cat# PS1-10G-10, lot# Q210-2) dissolved in assay buffer, the plate was centrifuged at 187 g for 30 s and incubated in the dark for 30 min. 2 µL of a mix of 200 µM ATP, 45 nM peptide (PerkinElmer; ULight™ phospho-40S-ribosomal protein S6 peptide; cat# TRF0129-D; lot# 1908909)) and 4 nM antibody (PerkinElmer; Eu-anti-phosph-rpS6, cat# TRF0217-D, lot# 1759011) were added and the plate was again centrifuged at 187 g for 30 s and incubated in the dark for 30 min. The FRET was measured on a Envision plate reader (excitation: 337 nm, emission filter donor: 615 nm, emission filter: acceptor 665 nm).

In situ testing of kinase inhibitors

To evaluate inhibitor effect on cell proliferation MV4-11, U937 and Ba/F3 cell lines were grown in RPMI, supplemented with 10% fetal bovine serum in an incubator at 37°C under 5% CO_2 atmosphere. Ba/F cells (wild-type) were grown in the presence of IL-3 (10 ng/mL, PeproTech). For viability assays, 10,000 cells were seeded per well in a 96-wells plate and inhibitors were added at the indicated concentration. After three days, cell viability was measured using the Cell Titer Blue (alamarBlue) viability assay (Promega) and fluorescence was measured using

the Clariostar (BMG Labtech). Relative survival was normalized to the untreated control and corrected for background signal. Data was processed using Microsoft Excel 2016, pIC_{50} values were fitted using GraphPad Prism 7.0. Experiments were performed in either n=3 or n=2.

References

(1) Shipley, J. L.; Butera, J. N. Acute Myelogenous Leukemia. *Exp. Hematol.* **2009**, *37* (6), 649–658.

(2) Döhner, H.; Weisdorf, D. J.; Bloomfield, C. D. Acute Myeloid Leukemia. *N. Engl. J. Med.* **2015**, *373* (12), 1136–1152.

(3) Stirewalt, D. L.; Radich, J. P. The Role of FLT3 in Haematopoietic Malignancies. *Nat. Rev. Cancer* **2003**, *3* (9), 650–665.

(4) Lange, B.; Valtieri, M.; Santoli, D.; Caracciolo, D.; Mavilio, F.; Gemperlein, I.; Griffin, C.; Emanuel, B.; Finan, J.; Nowell, P. Growth Factor Requirements of Childhood Acute Leukemia: Establishment of GM-CSF-Dependent Cell Lines. *Blood* **1987**, *70* (1), 192–199.

(5) Griffith, J.; Black, J.; Faerman, C.; Swenson, L.; Wynn, M.; Lu, F.; Lippke, J.; Saxena, K. The Structural Basis for Autoinhibition of FLT3 by the Juxtamembrane Domain. *Mol. Cell* **2004**, *13* (2), 169–178.

(6) Grunwald, M. R.; Levis, M. J. FLT3 Inhibitors for Acute Myeloid Leukemia: A Review of Their Efficacy and Mechanisms of Resistance. *Int. J. Hematol.* **2013**, *97* (6), 683–694.

(7) Fathi, A. T.; Chen, Y.-B. The Role of FLT3 Inhibitors in the Treatment of FLT3-Mutated Acute Myeloid Leukemia. *Eur. J. Haematol.* **2017**, *98* (4), 330–336.

(8) Levis, M. Midostaurin Approved for FLT3-Mutated AML. *Blood* **2017**, *129* (26), 3403–3406.

(9) Stone, R. M.; Manley, P. W.; Larson, R. A.; Capdeville, R. Midostaurin: Its Odyssey from Discovery to Approval for Treating Acute Myeloid Leukemia and Advanced Systemic Mastocytosis. *Blood Adv.* **2018**, *2* (4), 444–453.

(10) Kindler, T.; Lipka, D. B.; Fischer, T. FLT3 as a Therapeutic Target in AML: Still Challenging after All These Years. *Blood* **2010**, *116* (24), 5089–5102.

(11) Man, C. H.; Fung, T. K.; Ho, C.; Han, H. H. C.; Chow, H. C. H.; Ma, A. C. H.; Choi, W. W. L.; Lok, S.; Cheung, A. M. S.; Eaves, C.; et al. Sorafenib Treatment of FLT3-ITD+ Acute Myeloid Leukemia: Favorable Initial Outcome and Mechanisms of Subsequent Nonresponsiveness Associated with the Emergence of a D835 Mutation. *Blood* **2012**, *119* (22), 5133–5143.

(12) Smith, C. C.; Zhang, C.; Lin, K.; Lasater, E. A.; Zhang, Y.; Massi, E.; Damon, E.; Pendleton, M.; Bashir, A.; Sebra, R.; et al. Characterizing and Overriding the Structural Mechanism of the Quizartinib-Resistant FLT3 “Gatekeeper” F691L Mutation with PLX3397. *Cancer Discov.* **2015**, *5* (6), 668–679.

(13) Smith, C. C.; Wang, Q.; Chin, C.-S.; Salerno, S.; Damon, L. E.; Levis, M. J.; Perl, A. E.; Travers, K. J.; Wang, S.; Hunt, J. P.; et al. Validation of ITD Mutations in FLT3 as a Therapeutic Target in Human Acute Myeloid Leukaemia. *Nature* **2012**, *485* (7397), 260–263.

(14) Yamamoto, Y.; Kiyoi, H.; Nakano, Y.; Suzuki, R.; Kodera, Y.; Miyawaki, S.; Asou, N.; Kuriyama, K.; Yagasaki, F.; Shimazaki, C.; et al. Activating Mutation of D835 within the

Activation Loop of FLT3 in Human Hematologic Malignancies. *Blood* **2001**, *97* (8), 2434–2439.

(15) Sundström, C.; Nilsson, K. Establishment and Characterization of a Human Histiocytic Lymphoma Cell Line (U-937). *Int. J. Cancer* **1976**, *17* (5), 565–577.

(16) Warmuth, M.; Kim, S.; Gu, X.; Xia, G.; Adria, F. Ba / F3 Cells and Their Use in Kinase Drug Discovery ´ N. **2007**, 55–60.

(17) Daley, G. Q.; Baltimore, D. Transformation of an Interleukin 3-Dependent Hematopoietic Cell Line by the Chronic Myelogenous Leukemia-Specific P210bcr/abl Protein. *Proc. Natl. Acad. Sci. U. S. A.* **1988**, *85* (23), 9312–9316.

(18) Kelly, L. M.; Liu, Q.; Kutok, J. L.; Williams, I. R.; Boulton, C. L.; Gilliland, D. G. FLT3 Internal Tandem Duplication Mutations Associated with Human Acute Myeloid Leukemias Induce Myeloproliferative Disease in a Murine Bone Marrow Transplant Model. *Blood* **2002**, *99* (1), 310–318.

(19) Degorce, F.; Card, A.; Soh, S.; Trinquet, E.; Knapik, G. P.; Xie, B. HTRF: A Technology Tailored for Drug Discovery - a Review of Theoretical Aspects and Recent Applications. *Curr. Chem. Genomics* **2009**, *3*, 22–32.

(20) Baell, J. B.; Nissink, J. W. M. Seven Year Itch: Pan-Assay Interference Compounds (PAINS) in 2017—Utility and Limitations. *ACS Chem. Biol.* **2018**, *13* (1), 36–44.

(21) Baell, J.; Walters, M. A. Chemistry: Chemical Con Artists Foil Drug Discovery. *Nature* **2014**, *513* (7519), 481–483.

(22) O'Brien, J.; Wilson, I.; Orton, T.; Pognan, F. Investigation of the Alamar Blue (Resazurin) Fluorescent Dye for the Assessment of Mammalian Cell Cytotoxicity. *Eur. J. Biochem.* **2000**, *267* (17), 5421–5426.

(23) Nakayama, G. R.; Caton, M. C.; Nova, M. P.; Parandoosh, Z. Assessment of the Alamar Blue Assay for Cellular Growth and Viability in Vitro. *J. Immunol. Methods* **1997**, *204* (2), 205–208.